Chemical Response of the Upper Atmosphere due to Lightning-induced Electron Precipitation

Wei Xu,[1] Robert A. Marshall,[1] Antti Kero,[2] and Austin Sousa[1]

[1]Ann and H. J. Smead Department of Aerospace Engineering Sciences, University of Colorado Boulder, Boulder, Colorado, USA.
[2]Sodankylä Geophysical Observatory, University of Oulu, Oulu, Finland.

Key Points:

- We quantify the direct effects via excess odd hydrogen production on the middle atmosphere ozone layer produced by lightning-induced electron precipitation
- The change in ozone concentration (75–85 km altitude) during one thunderstorm via LEP processes is comparable to other types of energetic particle precipitation
- The long-term global chemical effects produced by LEP events are uncertain and need to be properly quantified

Corresponding author: Wei Xu, Wei-Xu@colorado.edu

Abstract

Terrestrial lightning frequently serves as a loss mechanism for energetic electrons in the Van Allen radiation belts, leading to lightning-induced electron precipitation (LEP). Regardless of the specific causes, energetic electron precipitation from the radiation belts in general has a significant influence on the ozone concentration in the stratosphere and mesosphere. The atmospheric chemical effects induced by LEP have been previously investigated using subionospheric VLF measurements at Faraday station, Antarctica (65.25°S, 64.27°W, L = 2.45). However, there exist large variations in the precipitation flux, ionization production, and occurrence rate of LEP events depending on the peak current of the parent lightning discharge, as well as the season, location, and intensity of the thunderstorm activity. These uncertainties motivate us to revisit the calculation of atmospheric chemical changes produced by LEP. In this study, we combine a well-validated LEP model and first-principles atmospheric chemical simulation, and investigate three intense storms in the year of 2013, 2015, and 2017 at the magnetic latitude of 50.9°, 32.1°, and 35.7°, respectively. Modeling results show that the LEP events in these storms can cumulatively drive significant changes in the NO_x, HO_x, and O_x concentration in the mesosphere. These changes are as high as ~156%, ~66%, and −5% at 75–85 km altitude, respectively, and comparable to the effects typically induced by other types of radiation belt electron precipitation events. Considering the high occurrence rate of thunderstorms around the globe, the long-term global chemical effects produced by LEP events need to be properly quantified.

1 Introduction

The concept of terrestrial lightning discharge as a loss mechanism for energetic electrons in the Van Allen radiation belts was first speculated by *Dungey* [1963], and later confirmed by direct measurements from the S81-1 (SEEP) satellite [*Voss et al.*, 1984, 1998]. This phenomenon is referred to as Lightning-induced Electron Precipitation (LEP), in which the Very-Low-Frequency (VLF, 3-30 kiloHertz, kHz) waves emitted from a lightning discharge propagate in the whistler mode through the Earth's magnetosphere, scatter energetic electrons into lower mirroring altitudes in the radiation belts, and ultimately cause the precipitation of some trapped electrons into the upper atmosphere. As a strong coupling between the Earth's atmosphere and magnetosphere, LEP has been the main focus of various observational studies [e.g., *Clilverd et al.*, 2002; *Rodger*, 2003; *Peter and Inan*, 2007; *Inan et al.*, 2010] in the past few decades. Even long before the first spacecraft measurements, LEP has been investigated using radio measurements [*Helliwell et al.*, 1973; *Rycroft*, 1973; *Lohrey and Kaiser*, 1979]. The most effective approach of LEP observation is via the indirect measurements of ionospheric electron density enhancements using subionospheric VLF remote sensing. VLF waves radiated from the Naval transmitters are well trapped within the waveguide formed between the ground and the sharp boundary in the lower ionosphere, and thus particularly sensitive to the electron density in the D-region ionosphere (~60–90 km), a region that is frequently bombarded by LEP fluxes.

A major goal of previous and ongoing VLF observations is to estimate the size, fluxes, and spectra of LEP events, and thereby quantify the effects of terrestrial lightning on the radiation belt fluxes. Many of the pioneer works have been carried out by *Inan et al.* [1985]; *Inan and Carpenter* [1986, 1987]. The authors revealed that the phase and amplitude perturbations of VLF signals associated with LEP events (historically known as Trimpi events [*Helliwell et al.*, 1973]), in most cases, can be explained using a whistler-induced precipitation flux ranging from 10^{-4} to 10^{-2} erg/cm^2/s. Using simultaneous measurements from multiple ground receivers, the size of LEP events has been estimated, by *Johnson et al.* [1999] and *Clilverd et al.* [2002], to be as large as one thousand kilometers overhead the causative lightning discharge. *Clilverd et al.* [2004] have further studied the relationship between VLF perturbations and the peak current of the source lightning flashes, and pointed out that the amplitude change of typical Trimpi events is consistent with lightning peak currents of 70–

250 kA. *Rodger et al.* [2005] have estimated the energy deposition via the LEP process into the middle atmosphere; a mean rate of energy deposition at L = 1.9–3.5 was found to be 3×10^{-4} erg/cm^2/min, with highs of 6×10^{-3} ergs/cm^2/min above North America. Studies using the Holographic Array for Ionospheric/Lightning Research (HAIL) found that, for a 100-kA lightning discharge, the peak flux of precipitation electrons is on the order of 10^{-2} ergs/cm^2/s [*Peter and Inan*, 2007]. In general, the spatial scale of lightning-induced electron precipitation ranges from several hundreds to one thousand kilometers, covering several degrees in latitude/longitude [e.g., *Clilverd et al.*, 2002]. As derived from ground VLF measurements, the displacement with respect to the lightning source is largely controlled by the geomagnetic field line, but primarily poleward shifted [e.g., *Peter and Inan*, 2007]. Lightning-generated whistler waves can lead to precipitation of energetic electron from both the inner and outer radiation belts: LEP events have been found to play a significant role in electron losses in the inner radiation belt [e.g., *Bortnik et al.*, 2006a,b; *Claudepierre et al.*, 2020a,b]; LEP can also lead to electron losses from the outer radiation belt, for example, Trimpi events [*Helliwell et al.*, 1973].

Due to the indirect relationship between VLF perturbations and the underlying D-region electron density variation, quantification of LEP fluxes using VLF measurements is by nature a nonlinear problem [*Marshall et al.*, 2019b]. The amplitude and phase changes of transmitter VLF signals are controlled not solely by the electron density enhancement, but also by the geometry of the transmitter-receiver path, the ambient ionosphere along the path [e.g., *Xu et al.*, 2019], and the collision frequency profile driven by the background atmosphere [*Marshall*, 2012]. As such, the LEP fluxes as inversely derived from VLF measurements are inherently ambiguous, with large uncertainties in the energy spectrum in particular. Besides VLF technique, LEP fluxes have been directly measured by in situ particle instruments, for example, the Solar Anomalous and Magnetospheric Particle Explorer (SAMPEX) [*Blake et al.*, 2001] and the Detection of Electro-Magnetic Emissions Transmitted from Earthquake Regions (DEMETER) satellite [*Inan et al.*, 2007]. However, nearly all existing space-borne instruments can only resolve part of the loss cone angle [*Marshall et al.*, 2020] and these measurements only provide a coarse estimate of the true precipitating flux.

Regardless of the specific causes, energetic electron precipitation (EEP) into the Earth's atmosphere, in general, has a significant influence on the ozone concentration in the upper atmosphere [e.g., *Thorne*, 1980; *Randall et al.*, 2007; *Sinnhuber et al.*, 2012] through the catalytic cycles of odd nitrogen (NO_x = [N] + [NO] + [NO_2]) [*Rusch et al.*, 1981] and odd hydrogen ([HO_x] = [H] + [OH] + [HO_2]) [*Solomon et al.*, 1981]. Using 60 major EEP events measured during the solar cycle 23, *Andersson et al.* [2014a] revealed that EEP strongly affects the ozone concentration and can cause up to 90% depletion at altitudes of 60–80 km. *Turunen et al.* [2016] have studied the chemical changes during a pulsating aurora event on November 17, 2012, and found a maximum reduction of 14% in ozone concentration at 75 km altitude. As for the chemical effects of LEP, *Rodger et al.* [2007] have performed detailed atmospheric chemistry simulations using the mean LEP energy flux reported in *Rodger et al.* [2005], but rescaled using the Trimpi events observed at Faraday station, Antarctica (65.25°S, 64.27°W, L = 2.45) on April 14, 1994. The maximum changes in NO_x and HO_x concentration were found to be ~0.1% around 80 km altitude, with a reduction of odd oxygen concentration by less than 0.1%, and thus the atmospheric chemistry effects were concluded to be insignificant [*Rodger et al.*, 2007].

However, there exist large variations in the precipitation flux, ionization production, and occurrence rate of LEP events depending on the peak current of the parent lightning discharge, as well as the season, location, and intensity of thunderstorm activity [*Sousa*, 2018]. For example, Figure 1 shows the comparison of ionization production between the mean LEP ionization production used by *Rodger et al.* [2005]; *Rodger et al.* [2007], and our more recent LEP modeling results [*Marshall et al.*, 2019a]. The colored lines (color-coded using time) show the ionization rate versus altitude produced by an LEP event over the first 10 seconds after a 100-kA lightning discharge at 35° magnetic latitude, as calcu-

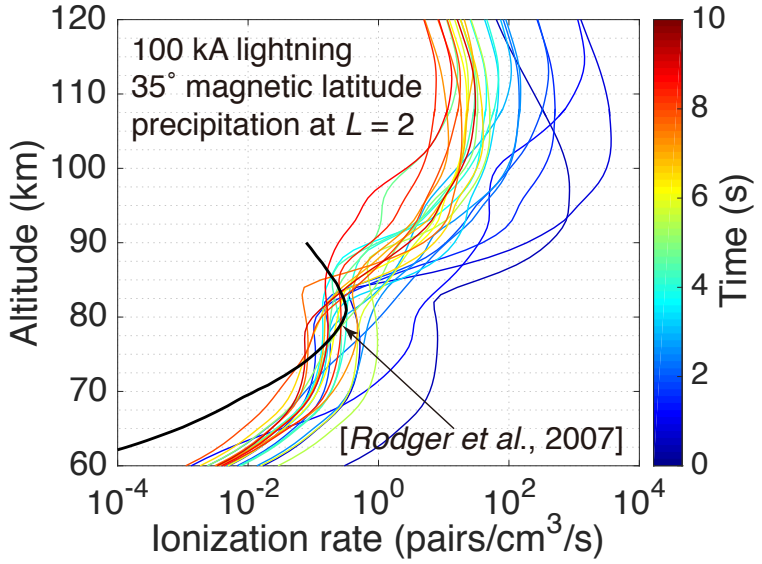

Figure 1. Comparison of the ionization production by lightning-induced electron precipitation between recent LEP modeling results [*Marshall et al.*, 2019a] using the WIPP code [*Lauben et al.*, 1999; *Bortnik*, 2004; *Sousa*, 2018] and the mean LEP ionization production [*Rodger et al.*, 2005; *Rodger et al.*, 2007]. The colored lines show the altitude profile of ionization production at $L = 2$ by a lightning source with a peak current of 100 kA at 35° magnetic latitude.

lated using the Stanford Wave-Induced Particle Precipitation (WIPP) code [*Lauben et al.*, 1999; *Bortnik*, 2004; *Golden et al.*, 2010; *Sousa*, 2018]. This code explicitly simulates from first principles the entire LEP process from the source lightning discharge to precipitation fluxes in the upper atmosphere. This model framework has been extensively used to analyze LEP-associated VLF measurements [e.g., *Peter and Inan*, 2007; *Inan et al.*, 2010], and more recently calibrated using X-ray measurements by the Balloon Array for Radiation-belt Relativistic Electron Losses (BARREL) during possible LEP events [*Marshall et al.*, 2019a]. In the first ~5 seconds, the mean LEP ionization production used by *Rodger et al.* [2007] (possibly corresponding to a peak current smaller than 100 kA) is on average one order of magnitude lower than that produced by this simulated 100-kA lightning discharge [*Marshall et al.*, 2019a].

Another parameter that is critical for LEP-induced chemical effects is the occurrence rate of intense lightning flashes. The flash rate was estimated to be approximately 3.3 events per minute for the Trimpi measurements at the Faraday station on April 14, 1994 [*Rodger et al.*, 2007]. A reexamination using the U.S. National Lightning Detection Network (NLDN) data [*Cummins et al.*, 1998] reveals that this value is not representative of intense thunderstorms at lower latitudes. As will be shown in section 3, the flash rate of lightning discharges with peak current larger than 50 kA could be as high as ~50 per minute, as observed during an intense thunderstorm occurring around 23.5°N, 97.5°W on October 25, 2015 (see Figure 3). In addition, the duration of a single LEP event was assumed to be ~0.2 s [*Rodger et al.*, 2007] in the ducted case, whereas it can last up to 20 seconds or longer in the non-ducted case [*Bortnik*, 2004; *Marshall et al.*, 2019a] due to multiple magnetospheric reflections between the conjugate hemispheres. Considering the high occurrence rate of LEP events (nearly once per minute globally) and potential chemical effects, the uncertainties in the LEP source (mostly from the uncertainties about the peak current of source lightning discharge, energy and pitch angle distribution of precipitation fluxes) motivate us to revisit the calculation of atmospheric chemical changes. In this paper, we present first-principles

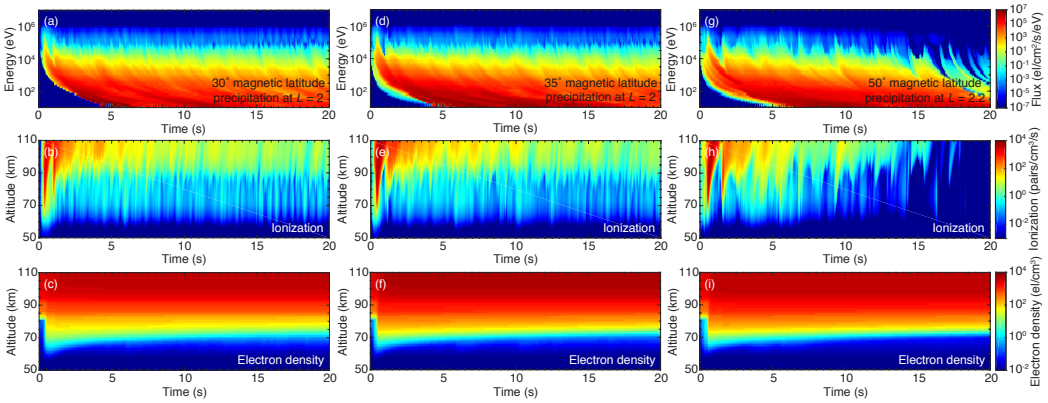

Figure 2. (a) Differential flux of precipitation electrons with energies between 10 eV and 10 MeV at $L = 2$ due to a 100 kA lightning source at 30° magnetic latitude. (b) Ionization production at altitudes between 50 and 110 km by these precipitation electrons. The background atmospheric profile used in this ionization calculation is obtained using the date, latitude, and longitude of the 2015 storm reported by NLDN (see section 3). (c) Electron density change in the D-region ionosphere produced by this LEP event. Panels (d–f) show similar results, but for a lightning source at 35° magnetic latitude and precipitation fluxes at $L = 2$. Panels (g–i) show the results for a lightning source at 50° magnetic latitude and precipitation fluxes at $L = 2.2$. The background atmospheric profile used for the ionization calculation of panel (e) and (h) is obtained using the date and location of the 2017 and 2013 storm (see section 3), respectively.

modeling results of LEP events, including the precipitation fluxes, ionization production, and chemical changes. We use three NLDN-reported intense storms as extreme examples to quantify the chemical effects produced by LEP.

2 Numerical Simulations

In this study, we combine the WIPP-LEP simulations of lightning-induced electron precipitation [*Lauben et al.*, 1999; *Bortnik*, 2004; *Sousa*, 2018], the Boulder Electron Radiation to Ionization (BERI) model [*Xu et al.*, 2020], and the Sodankylä Ion and Neutral Chemistry (SIC) model [*Turunen et al.*, 1996; *Verronen et al.*, 2005], specifically in three steps. First, following the framework formulated by *Lauben et al.* [1999]; *Bortnik* [2004], the WIPP model is employed to simulate LEP events produced by source lightning discharges at different magnetic latitudes and calculate the resultant precipitation fluxes at different observation locations (L values). Second, three intense storms are picked from the NLDN database for the years of 2013–2017 at the magnetic latitudes of 30°–50°. Using the WIPP results obtained in the first step, we calculate the total ionization production by the precipitation fluxes induced by all lightning flashes in these storms (denoted as the cumulative ionization production hereafter). Finally, the cumulative ionization production is utilized as an external forcing in SIC simulations in order to quantify the atmospheric changes to constituents of interest. Similar to previous EEP studies [*Turunen et al.*, 1996, 2009], the main focus of this study is the relative change in the molecular concentration of odd hydrogen, odd nitrogen, and odd oxygen ($[O_x] = [O] + [O_3]$). In the following, we introduce the numerical models and the initial parameters used in these simulations.

The WIPP code was built upon the modeling work of *Inan* [1977], and has been refined through the past three decades of LEP modeling work at Stanford by *Lauben et al.* [1999]; *Bortnik* [2004]; *Golden et al.* [2010]; *Cotts* [2011]; *Sousa* [2018]. The details of this code, as well as the most recent updates, can be found in *Sousa* [2018]. In short, a stan-

dard WIPP-LEP simulation includes four steps [*Bortnik*, 2004; *Sousa*, 2018; *Marshall et al.*, 2019a]: i) The electromagnetic pulse (EMP) energy emitted by the return stroke current of a lightning discharge is calculated and mapped to the base of the ionosphere at 100 km altitude, ii) We calculate the attenuation of lightning-emitted VLF waves during their propagation through the lossy ionosphere (100–1000 km altitude) using the VLF attenuation curves [*Helliwell*, 1965; *Graf et al.*, 2013a], iii) Starting from 1000 km altitude, the propagation of each frequency component in the plasmasphere is simulated using the improved Stanford ray-tracing program [*Bortnik et al.*, 2006a; *Golden et al.*, 2010]. Each ray is tracked through the plasmasphere for 20 seconds due to multiple magnetospheric reflections, iv) We calculate the resonant wave-particle interactions between these waves and the radiation belt fluxes, and mainly focus on the modification to the pitch angles of trapped electrons near the loss cone edge.

The fluxes and spectra of radiation belt electrons are calculated using the AE8 model [*Vette*, 1991] and their pitch angles are assumed to be sine-distributed between 0° and 90° [*Sousa*, 2018; *Marshall et al.*, 2019a]. Note that precipitation fluxes are strongly dependent on the assumption of the background fluxes and pitch angle distributions; the most important part of pitch angle distribution is the region near the loss cone angle; the uncertainty brought by the assumption of pitch angle distribution has been previously discussed in *Marshall et al.* [2019a]; our results were validated using Van Allen Probes data, as reported in *Marshall et al.* [2019a]. WIPP simulations are performed for lightning discharges at magnetic latitudes between 15° and 55° with 5° steps. For each magnetic latitude, the differential fluxes of precipitation electrons with energies between 10 eV and 10 MeV are calculated for different observation locations (L values). To quantify the maximum chemical effects, the location with the highest precipitation flux (as denoted in the upper panels of Figure 2) is used to calculate the ionization production and resultant chemical changes. It is important to emphasize that in the WIPP simulations, the precipitation fluxes scale linearly with the total input EMP energy, which is proportional to the square of lightning peak current. Following this relation, WIPP-calculated LEP fluxes can be readily rescaled to the NLDN-reported peak current. This relation is close to that empirically determined by *Clilverd et al.* [2004], wherein the precipitation flux scales as the 2.3 power of lightning peak current.

Knowing the precipitation fluxes, we calculate the ionization production at altitudes below 150 km altitude (the upper boundary of the SIC model) using the BERI model [*Xu et al.*, 2020]. This model is largely based on a lookup table of atmospheric ionization production by monoenergetic electrons with energies between 3 keV and 33 MeV, and pitch angles between 0° and 90°. This lookup table was developed using physics-based Monte Carlo simulations [e.g., *Lehtinen et al.*, 1999; *Xu and Marshall*, 2019], and allows rapid and accurate specification of ionization production by arbitrary precipitation energy and pitch angle distribution in any atmospheric condition. In this study, it is assumed that the precipitation electrons of each LEP burst at 500 km altitude are isotropically distributed in pitch angles between 0° and 90°. The mass density profile of background atmosphere is calculated using the NRLMSISE-00 model [*Tobiska and Bouwer*, 2006] for the date, latitude, and longitude of the storms reported by NLDN (see section 3).

Figure 2a shows WIPP modeling results of precipitation fluxes at L = 2 produced by a 100-kA lightning discharge at the magnetic latitude of 30°. The two peaks at ~0.4 s and ~1 s, as typical of satellite measurements of LEP events [*Voss et al.*, 1998], are caused by the interaction between radiation belt electrons and the initial upward-going whistler waves and the reflected whistler waves, respectively. The ionization production by these precipitation electrons at altitudes between 50 and 110 km is shown in Figure 2b. The background atmospheric profile used in this ionization calculation is obtained using the date, latitude, and longitude of the 2015 storm reported by NLDN (see Figure 3). Using a 5-species chemistry model [*Glukhov et al.*, 1992; *Lehtinen and Inan*, 2007], we have further calculated the electron density change in the D-region ionosphere, as shown in Figure 2c. Figures 2d–2f show similar results, but for a lightning source at 35° magnetic latitude and precipitation

fluxes at L = 2, while Figures 2g–2i show those for a lightning source at 50° magnetic latitude and precipitation fluxes at L = 2.2. The background atmospheric profile used for the calculation of Figure 2e and Figure 2h is obtained using the date and location of the 2017 and 2013 storm (see section 3), respectively. Of note, the electron density variations shown in the bottom panels of Figure 2 are capable of reproducing the typical amplitude changes (~0.5–2 dB) of transmitter VLF signal during LEP events [*Peter and Inan*, 2007]. Moreover, the peak precipitation flux produced by the lightning discharge at 30°, 35°, and 50° latitude is 0.06, 0.14, and 0.15 ergs/cm^2/s, somewhat higher but not unreasonably different from the values suggested by *Peter and Inan* [2007].

Because of the dense electron density in the D- and E-region ionosphere, the lightning EMP energy is severely attenuated during the daytime ionospheric conditions [*Graf et al.*, 2013b] and the resultant precipitation fluxes are considerably lower than nighttime [*Sousa*, 2018]. Therefore, in this study, we mainly focus on those thunderstorms with high flash rates and large peak currents, occurring during local nighttime conditions. Given these criteria, three intense storms were chosen from NLDN data for the years of 2013, 2015, and 2017 at the magnetic latitudes of 50.9°, 32.1°, and 35.7°, respectively. The geolocation, temporal evolution, and peak current of lightning flashes in these storms are presented in section 3.

The total ionization production during a thunderstorm is a key parameter in chemical simulations, and is calculated using all the flashes with peak current larger than 50 kA in the present study. A minimum value of 50 kA is used since it is close to what is needed to trigger Trimpi events (70 kA) with detectable ionosphere enhancements [*Clilverd et al.*, 2004]. *Clilverd et al.* [2002] also noted that, if the lightning peak current is less than 45 kA, the chance of observing any Trimpi events is almost zero. We have checked that, if a lower threshold value is instead used, the cumulative ionization production would not change significantly since the LEP flux scales linearly with the square of lightning peak current. Specifically, for a given storm, we use the WIPP results at the corresponding magnetic latitude (upper panels of Figure 2) and rescale the ionization results (middle panels of Figure 2) using the peak current of all NLDN-reported lightning flashes ($\geq$ 50 kA). The rescaled ionization production is then sorted using the NLDN-tagged time of each flash (see Figure 3b). Finally, these ionization results are summed together and we calculate the cumulative ionization production versus altitude and time for each storm (see Figure 3c).

The cumulative ionization production is then used as an input into SIC chemistry simulations. SIC is a 1-D atmospheric model that dynamically solves for the concentration of 16 minor neutral species and 72 ionic species in the altitude range between 20 and 150 km with 1 km resolution [*Turunen et al.*, 1996; *Verronen et al.*, 2005; *Verronen*, 2006]. Vertical motion of species is included as molecular and eddy diffusion, neglecting transport by prevailing neutral winds. The latest version of this model takes into account 389 ion-neutral and neutral-neutral reactions, and 2523 ion-ion and electron-ion recombination reactions. The background profile of neutral density used in SIC modeling is obtained from the NRLMSISE-00 model [*Tobiska and Bouwer*, 2006] using the daily average values of solar radio flux ($F_{10.7}$) and the geomagnetic activity index (A_p). Note that horizontal mixing is not included in the 1-D SIC model; this effect will be investigated in our next-step study using global circulation simulations.

In this study, the neutral density profile is calculated using the specific date and location of each storm as reported by NLDN. Solar proton precipitation is provided as an optional external force in the SIC model, but not included in present simulations. The initial profiles of HO_x, NO_x, O_x are obtained by running the SIC model at the thunderstorm location for 5 days, prior to the LEP forcing with photoionization only. Chemical changes are simulated for a period of 24 hours starting from the first LEP event and stored every 1 minute of simulation. An average ionization rate of the event is used. Two sets of SIC simulations are performed for each storm, one with and another without the LEP-induced ionization production. The simulation results obtained without applying LEP ionization are regarded as

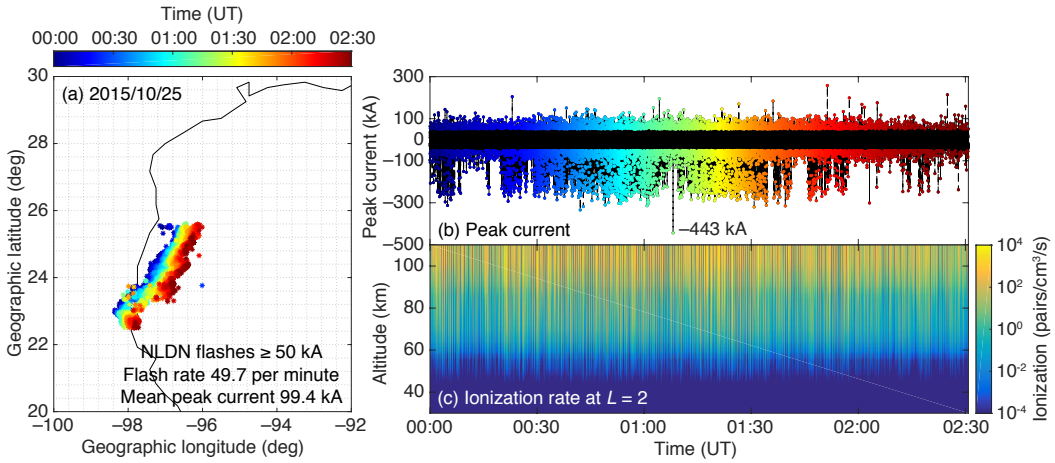

Figure 3. NLDN measurements of lightning flashes between ~00:00 and ~02:30 UT on October 25, 2015 near 23.5°N, 97.5°W. (a) Longitude and latitude of all lightning flashes with peak current magnitude larger than 50 kA. The rate of lightning flashes with peak current magnitude larger than 50 kA is ~49.7 flashes per minute and the average value of peak current for these flashes is ~99.4 kA. (b) Peak current of lightning flashes versus the occurrence time. The largest peak current recorded by NLDN was −443 kA at 01:08:08 UT. (c) Altitude profile of ionization production by the lightning flashes with peak current magnitude larger than 50 kA shown in panel (b).

the baseline, against which we compute the relative changes in neutral species and therefore quantify the chemical effects.

We emphasize that all above-mentioned numerical models have been well validated in previous studies. The WIPP code has been extensively used to interpret LEP-modulated VLF signals [e.g., *Peter and Inan*, 2007], and lately the X-ray fluxes recorded by BARREL during possible LEP events [*Marshall et al.*, 2019a]. Different from VLF measurements, X-ray measurements at balloon altitudes are directly linked to the precipitation fluxes and energy spectra of LEP bursts; WIPP results can fully explain the X-ray fluxes, temporal signature, and energy spectra measured by BARREL [*Marshall et al.*, 2019a]. As for the BERI model [*Xu et al.*, 2020], it shows good agreements with the parameterization method of *Fang et al.* [2010] in terms of the peak ionization rate and altitude, with a maximum difference of ~20% among tests using different precipitation energy and pitch angle distributions. The SIC model has been employed for the estimation of atmospheric chemical effects due to a wide variety of external sources, including radiation belt electron precipitation [e.g., *Turunen et al.*, 2016; *Xu et al.*, 2018], solar eclipse [e.g., *Xu et al.*, 2019], and solar proton events [e.g., *Clilverd et al.*, 2005].

3 Results

3.1 Storm 1: October 25, 2015

The first storm in this case study occurred on October 25, 2015 at geographic latitudes between 22.5°N and 25.6°N, and geographic longitudes between 96.0°W and 98.5°W, along the Caribbean coast of Texas / Mexico. Figure 3a shows the longitudes and latitudes of all lightning flashes with peak current magnitude larger than 50 kA recorded by the NLDN network between ~00:00 and ~02:30 UT, with color progressing in time from blue to red. The peak current and occurrence time of these lightning flashes are shown separately in Fig-

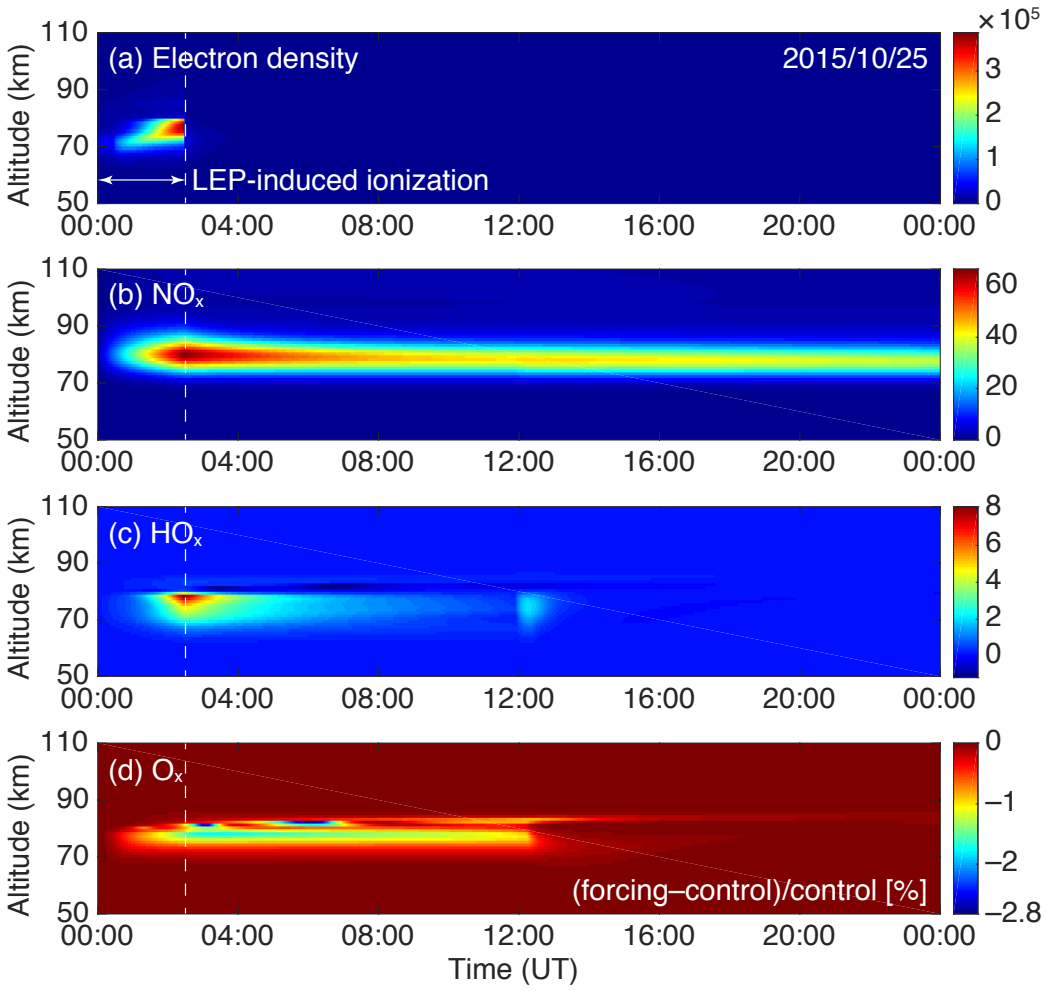

313 **Figure 4.** SIC modeling results of the relative changes in (a) electron, (b) NO_x, (c) HO_x, and (d) O_x
314 concentration produced by all the LEP events in the 2015 storm. Sunrise time: 12:30:27 UT. This figure
315 specifically shows the percentage difference between simulation results obtained with (denoted as forcing)
316 and without (denoted as control) applying the cumulative ionization production (Figure 3c). The cumulative
317 ionization production between 00:00 and 02:30 UT is marked using white dashed lines in these panels.

ure 3b. The black and colored dots show the lightning flashes with peak current magnitude smaller and larger than 50 kA, respectively.

NLDN reported a total of 33,504 flashes from this region between 00:00 and 02:30 UT, ~22.3% of which had peak current larger than 50 kA (7,453 flashes). The flash rate of intense lightning discharges (≥ 50 kA) was approximately 49.7 per minute. The average value of the peak current for these 7,453 flashes was ~99.4 kA and the majority were negative cloud-to-ground discharges. Out of the 33,504 flashes, the fraction of lightning flashes with peak current larger than 70 kA and 100 kA was approximately 11.2% (3,748 flashes) and 6.4% (2,157 flashes), respectively; the largest peak current was −443 kA at 01:08:08 UT, likely associated with large-scale high-altitude luminous events, for example, elves [e.g., *Marshall et al.*, 2010] or sprites [e.g., *Pasko et al.*, 1997].

The magnetic latitude corresponding to the center of this storm is approximately 32.1°N, as calculated using the International Geomagnetic Reference Field (IGRF) model [*Thébault et al.*, 2015]. Thus, the WIPP-calculated precipitation fluxes produced by the lightning discharge at 30° magnetic latitude (Figures 2a–2b) are used for the ionization calculation. The LEP-produced ionization profile in Figure 2b is rescaled using the peak current of the lightning flashes (colored dots with peak current ≥ 50 kA) shown in Figure 3b, sorted using the NLDN-tagged occurrence time (Figure 3b), and then summed together. Figure 3c shows the cumulative ionization production via all LEP processes during this 150-minute storm.

These ionization results are then used as the forcing input to the SIC model in order to calculate the atmospheric chemistry response. Figure 4, from top to bottom, presents the relative change in the concentration of electrons, NO_x, HO_x, and O_x produced by all the LEP events in storm 1. This figure specifically shows the percentage difference between the simulation results obtained with (denoted as forcing in Figure 4) and without (denoted as control in Figure 4) applying the cumulative ionization production during this storm ((forcing − control) / control ×100 [%]). The cumulative ionization production between 00:00 and 02:30 UT is marked using white dashed lines in this figure. The electron density is dramatically enhanced, by three orders of magnitude in the D-region ionosphere, as seen in Figure 4a. This level of electron density change is close to previously reported results [e.g., *Peter*, 2007, Figure 5.2]. The maximum change of NO_x concentration, due to the LEP-induced ionization, is approximately 67% at ~80 km altitude. NO_x is relatively stable and these changes can persist for a long time; about 37% of the excess NO_x production remains at the end of this 24-hour simulation period (see Figure 4b).

Different from NO_x, the HO_x change is considerably smaller and non-monotonic. HO_x concentration increases by ~8.1% at the altitudes near 78 km, and decreases by ~1.2% at 82 km altitude after the LEP forcing at ~06:52 UT. Above 82 km, the HO_x change is very small because of the limited abundance of water vapor in this altitude range [*Turunen et al.*, 2016]. A reduction of 2.8% is predicted for the O_x density around the local minimum in the mesospheric ozone profile, ~82 km altitude. However, because of the solar radiation and enhanced photochemistry during the sunrise [*Verronen*, 2006], the HO_x concentration is shortly enhanced (see Figure 4c) and the O_x concentration returns to the background value around ~12:00 UT (see Figure 4d).

3.2 Storm 2: August 22, 2013

Lightning at higher magnetic latitudes projects to higher *L*-shells in the radiation belts, and thus has the potential to impact fluxes in the heart of the radiation belts and produce more intense precipitation signatures. To investigate the LEP effects at higher latitudes, the second case study is performed for the thunderstorm occurring on August 22, 2013 at geographic latitudes between 41.8°N and 43.0°N, and longitudes between 96.5°W and 100.0°W, in northeastern Nebraska. Nebraska is well known for producing uncommonly intense positive lightning discharges [e.g., *Stolzenburg*, 1994]. The magnetic latitude of this storm is ~50.9°N and the NLDN lightning data from 01:34 to 04:54 UT are used. Similar to Fig-

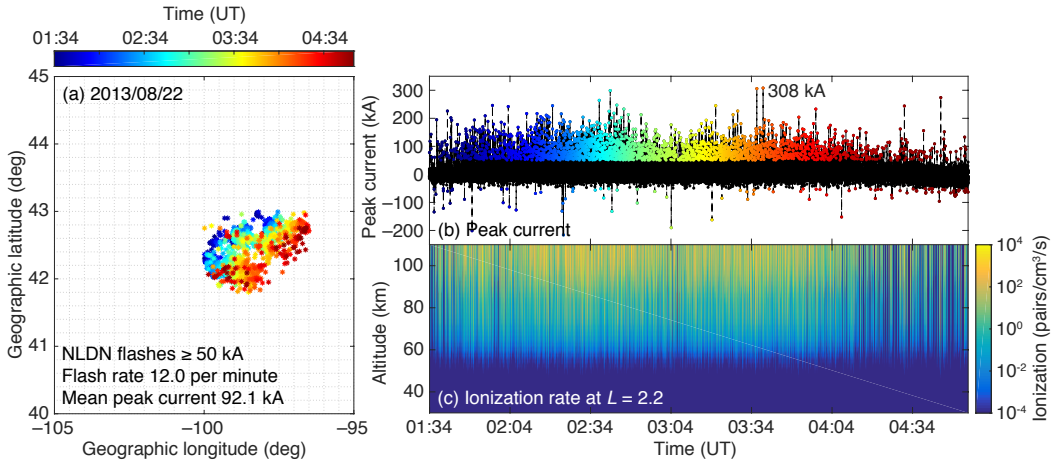

Figure 5. Similar to Figure 3, but for the NLDN-reported lightning flashes near 42.4°N, 98.7°W between 01:34 and 04:54 UT on August 22, 2013.

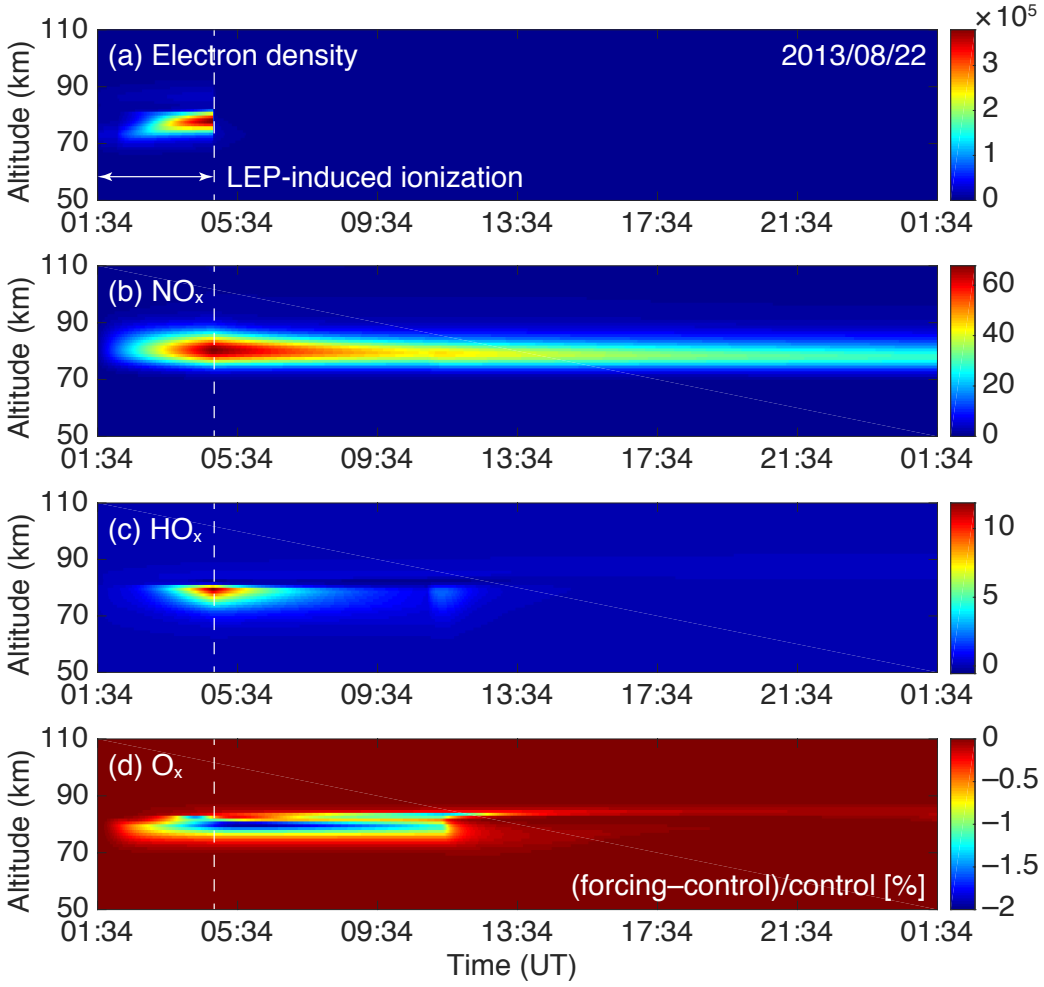

Figure 6. Similar to Figure 4, but for the NLDN-reported lightning flashes near 42.4°N, 98.7°W between 01:34 and 04:54 UT on August 22, 2013. Sunrise time: 11:51:14 UT.

ure 3, Figure 5a shows the temporal evolution of lightning flashes with peak current magnitude larger than 50 kA and Figure 5b shows the peak current versus occurrence time for these flashes. The WIPP results corresponding to a lightning source at 50° magnetic latitude (Figure 2h) are utilized for the calculation of cumulative ionization production, as shown in Figure 5c.

Compared to the baseline runs, the relative change in NO_x, HO_x, and O_x concentration is ~67%, ~12%, and −2%, respectively. The O_x change in this case is smaller than that of the first storm, the NO_x change is comparable, and the HO_x change is slightly higher. Note that the relative change of these neutral species is somewhat sensitive to the baseline conditions, for example, the season, location, and background atmospheric condition of baseline simulations. On average, the cumulative ionization production in the second storm is notably less than that of the first storm since the peak current and flash rate are lower. In the second storm, 2,390 lightning flashes with peak current larger than 50 kA were detected by NLDN and the flash rate was ~12.0 events per minute, a quarter of that for the first storm. The average value of peak current for these flashes (≥ 50 kA) was ~92.1 kA, which is also 7.3% lower than the first storm (99.4 kA). Out of these 2,390 flashes, the number of flashes with peak current larger than 70 kA and 100 kA was 1,585 and 775, respectively, and the largest peak current reported by NLDN was 308 kA.

Atmospheric chemical changes, in essence, are positively related with the cumulative ionization production during a thunderstorm for a given atmospheric condition, which is largely controlled by the LEP fluxes and lightning flash rate if the dependence on the precipitation energy spectrum is not considered. As explained in section 2, the precipitation flux of a single LEP event is linearly proportional to the square of lightning peak current. The lightning flash rate can enhance or diminish the cumulative effects of ionization production during a thunderstorm. Thus, these two parameters can be roughly considered as a proxy for the extent of ionization and chemical effects produced by thunderstorm activity via LEP processes. It is important to note that the fluxes of LEP bursts are also dependent on the L-shell from which lightning whistler induces electron precipitation, i.e., the availability of energetic electrons in the radiation belts, as well as their pitch angle distribution.

3.3 Storm 3: May 29, 2017

For completeness of this case study, a third storm is chosen at a magnetic latitude between the first two storms, at ~35.7°N. This storm took place on May 29, 2017 at geographic latitudes between 25.5°N and 28.2°N, and longitudes between 96.0°W and 100.5°W, near the U.S. and Mexico border along the Caribbean coast. The NLDN data between 04:29 and 09:59 UT are used for the chemistry simulation. The geolocation, peak current, and ionization production by the lightning flashes in this storm are shown in Figure 7. A total of 440,266 lightning flashes were identified by NLDN to originate from this storm, and the fraction of lightning discharges with peak current greater than 50 kA, 70 kA, and 100 kA was 2.5% (11,148 flashes), 0.9% (3,971 flashes), and 0.4% (1,753 flashes), respectively. These flashes were mostly negative cloud-to-ground discharges. The rate of lightning flashes with peak current larger than 50 kA was 33.8 flashes per minute, with the average value of the peak current (flashes ≥ 50 kA) being 77.6 kA and the largest value being 292 kA.

Given the NLDN-reported flash rate and peak current, it is not unexpected that this storm leads to the largest chemical changes among all cases, as evidenced in Figure 8. SIC modeling results show that LEP-induced ionization results in notable NO_x and HO_x changes: the NO_x concentration is more than doubled at altitudes between ~76 and ~84 km, with a maximum enhancement of 156% at ~80 km; the HO_x concentration increases by ~66% around 78 km altitude compared to the control runs. The O_x change in this case closely follows that of HO_x: at altitudes between ~77 and ~83 km, the O_x concentration reduces by more than ~3% and the maximum reduction is approximately 5% at 79 km altitude.

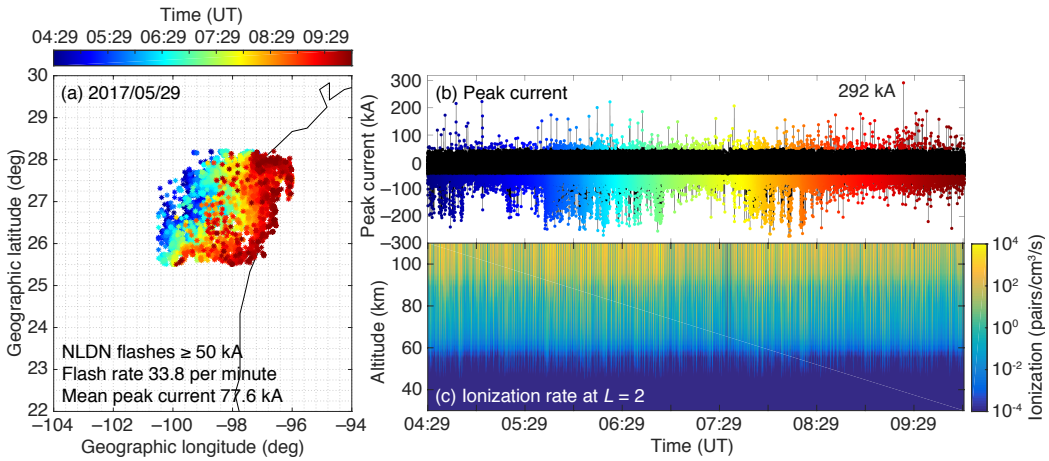

422 **Figure 7.** Similar to Figure 3, but for the NLDN-reported lightning flashes near 27.3°N, 98.3°W between
423 04:29 and 09:59 UT on May 29, 2017.

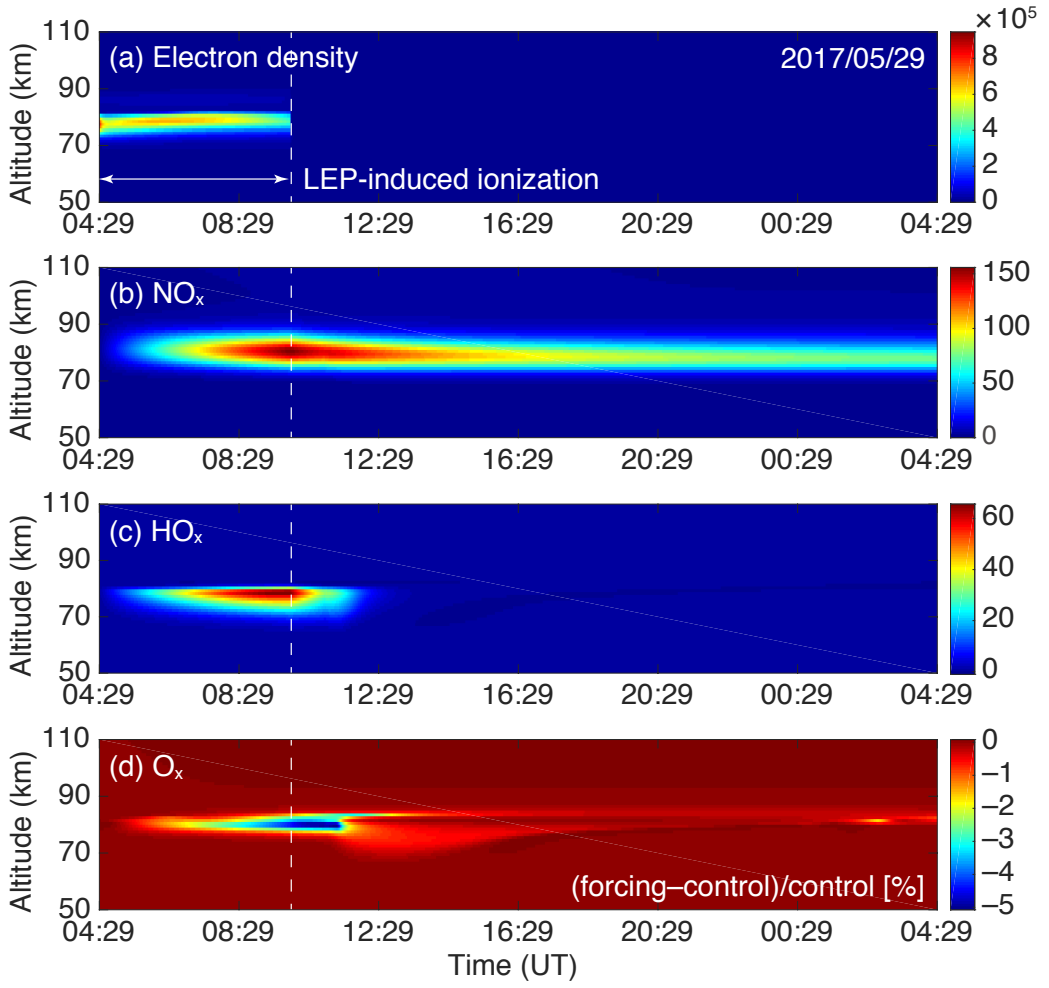

424 **Figure 8.** Similar to Figure 4, but for the NLDN-reported lightning flashes near 27.3°N, 98.3°W between
425 04:29 and 09:59 UT on May 29, 2017. Sunrise time: 11:42:58 UT.

4 Conclusion and Discussion

In this study, using a suite of well-validated LEP and atmospheric ionization models, we have calculated the precipitation fluxes and ionization production by lightning flashes at different magnetic latitudes. Case studies for three intense storms in the years from 2013 to 2017 at magnetic latitudes of 30°–50° are performed using NLDN-reported lightning data. Using SIC modeling of atmospheric changes, we have further quantified the relative changes in the electron, NO_x, HO_x, and O_x concentration due to the LEP events in these storms.

Because of LEP-induced ionization, the NO_x and HO_x concentration at altitudes between 75 and 85 km is enhanced by up to ~156% and ~66%, respectively, during these storms. The maximum reduction in ozone concentration is approximately 5%, as driven by the catalytic reaction cycles of HO_x. These atmospheric changes are one order of magnitude larger than those suggested by *Rodger et al.* [2007], mainly because of the variation in lightning flash rate and thunderstorm intensity. The mean LEP ionization production used by *Rodger et al.* [2007] was calculated using a mean precipitation energy flux of 2×10^{-3} ergs/cm^2/s [*Rodger et al.*, 2005], as required to explain Faraday Trimpi measurements. The chemical simulation of *Rodger et al.* [2007] was conducted using the Trimpi events observed at the Faraday station on April 14, 1994, corresponding to a Trimpi rate of 3.3 events per minute. However, as shown in section 3, the NLDN-reported lightning peak current and flash rate for the three storms reported herein are orders of magnitude higher.

We emphasize that the three storms investigated in this study do not represent the most intense cases on a global scale, albeit stronger than majority of the thunderstorm activity in North America. According to space-borne measurements of lightning activity, north and central Argentina is the region that hosts the most intense convective storms on the Earth [e.g., *Houze et al.*, 2015]. As outlined above, the atmospheric effects are positively related with the intensity of thunderstorm activity, and it is conceivable that the chemical effects of Argentinian storms could be even more dramatic. On the other hand, Argentinian storms occur at low magnetic latitudes, corresponding to the inner radiation belt, where the available fluxes of electrons for precipitation may be lower.

The main findings of our study are not contradictory to those of *Rodger et al.* [2007], but more complementary. The main difference between the ionization calculation of *Rodger et al.* [2007] and *Marshall et al.* [2019a] is that *Rodger et al.* [2007] modeled LEP events in the ducted case, while *Marshall et al.* [2019a] modeled the LEP process in the nonducted case due to multiple magnetospheric reflections; the energy and pitch angle distribution of LEP fluxes are different. The main focus of *Rodger et al.* [2007] is the average LEP effects produced by lightning discharge at high magnetic latitude, while this study mainly focuses on the LEP effects at relatively lower latitudes and in extreme cases, which have not been previously investigated. This study represents the first step of a series of studies towards better understanding on the atmospheric chemical effects brought by LEP. The main goal is to evaluate the immediate effects produced by LEP against other known ionization sources. The next-step study is to quantify the indirect effects produced by LEP events using a 3D global circulation model. Future studies can also aim at comparing the chemical effects reported in this study with ground- and/or space-based measurements.

A 5% ozone depletion at 75–85 km altitude is comparable to that brought by other EEP processes, for example, microburst precipitation [*Seppälä et al.*, 2018], EMIC-driven electron precipitation [*Hendry et al.*, 2021], as well as pulsating auroras [*Turunen et al.*, 2016]. Compared to other types of energetic particle precipitation (EPP), a single LEP event is considerably shorter in duration and lower in precipitation fluxes. LEP produced by a 100-kA lightning discharge has a peak energy flux ranging from 10^{-2} [*Peter and Inan*, 2007] to 10^{-1} ergs/cm^2/s [*Marshall et al.*, 2019a], while typical values for the precipitation flux associated with visible aurora are 0.1–10 ergs/cm^2/s [*Meng*, 1976; *Rees*, 1992]. Nevertheless, with thousands of lightning flashes repetitively occurring within a short time window of a

few hours, i.e., an intense thunderstorm, the cumulative effects are pronounced, and the ionization production and chemical changes become accordingly amplified.

An O_x change of several percent is more significant than it appears since the occurrence rate of LEP events globally is overwhelmingly higher than other EPP processes. The global lightning flash rate ranges from several tens to one hundred per second [*Rakov*, 2016], although not all flashes are sufficiently charged to give rise to radiation belt precipitation. Using Trimpi measurements, a representative value of the mean LEP rate at the Faraday station was found to be 0.79 per minute [*Rodger et al.*, 2004]. *Rodger et al.* [2003] have further estimated the global LEP rate using lightning observation data. An average value was suggested to be 0.18, 0.29, and 0.35 per minute at the L value of 2.4, 2, and 1.7, respectively. These values however, as noted by the authors, should only be considered as the lower bounds [*Rodger et al.*, 2003] since not all LEP events cause significant VLF changes, due to the interference of waveguide modes and the nonlinear relation between the electron density enhancement and VLF perturbation.

As in the 1D chemical simulation, the ozone reduction is mainly due to the immediate effects of HO_x variation. Because of self-dissociation, HO_x has a relatively short lifetime and its effects on the ozone concentration are highly localized in space and time [*Turunen et al.*, 2016]. *Andersson et al.* [2014b] have shown that the global distribution of nighttime OH is mostly influenced by EEP events at high latitudes, whereas lightning discharge and associated LEP event occur more frequently at low latitudes. As such, the ozone reduction due to HO_x changes produced by LEP events could be insignificant. Present results show that, due to LEP ionization, the NO_x concentration could be enhanced by as high as ~156% in the mesosphere, but their effects on the ozone layer are not captured by the present chemistry simulation. In the context of LEP events, the NO_x effects could become even greater than what is predicted in the present study for a single thunderstorm if we take the global occurrence rate into account, although lightning activity tends to be more intense and frequent during summer times at low- and mid-latitude regions [*Sousa*, 2018]. From this consideration, the long-term global chemical effects of LEP events may be potentially important, but have been largely overlooked in previous studies.

To quantify these effects, the ionization results presented in Figure 2 can be rescaled using the lightning peak current reported by real time lightning-monitoring network, for example, the World Wide Lightning Location Network (WWLLN) [*Dowden et al.*, 2002]. The lightning data can be converted into altitude profiles of ionization production by LEP events, and then incorporated into global atmospheric chemistry and transport models such as the Whole Atmosphere Community Climate Model (WACCM) [*Verronen et al.*, 2016]. Future studies can thereby take the latitudinal and seasonal variation of thunderstorm activity into account, and aim at assessing the long-term global chemical effects produced by LEPs.

Acknowledgments

This research was supported by the NSF MAG award #AGS1732359. The work of A. Kero is funded by the Tenure Track Project in Radio Science at Sodankylä Geophysical Observatory/University of Oulu. We sincerely thank Vaisala Inc. for providing the NLDN data. The simulation data and analysis codes used to generate all figures and results in this paper are available at https://doi.org/10.5281/zenodo.4599480.

References

Andersson, M., P. Verronen, C. Rodger, M. Clilverd, and A. Seppälä (2014a), Missing driver in the Sun–Earth connection from energetic electron precipitation impacts mesospheric ozone, *Nature communications*, *5*, 5197.

Andersson, M. E., P. T. Verronen, C. J. Rodger, M. A. Clilverd, and S. Wang (2014b), Longitudinal hotspots in the mesospheric OH variations due to energetic electron precipitation,

Atmospheric Chemistry and Physics, *14*(2), 1095–1105.

Blake, J. B., U. S. Inan, M. Walt, T. F. Bell, J. Bortnik, D. L. Chenette, and H. J. Christian (2001), Lightning-induced energetic electron flux enhancements in the drift loss cone, *J. Geophys. Res.*, *106*(A12), 29,733–29,744.

Bortnik, J. (2004), Precipitation of radiation belt electrons by lightning-generated magnetospherically reflecting whistler waves, Ph.D. thesis, Stanford University.

Bortnik, J., U. S. Inan, and T. F. Bell (2006a), Temporal signatures of radiation belt electron precipitation induced by lightning generated MR whistler waves. Part 1: Methodology, *J. Geophys. Res.*, *111*, A02204, doi:10.1029/2005JA011182.

Bortnik, J., U. S. Inan, and T. F. Bell (2006b), Temporal signatures of radiation belt electron precipitation induced by lightning-generated MR whistler waves: 2. Global signatures, *J. Geophys. Res.*, *111*, A02,205.

Claudepierre, S. G., Q. Ma, J. Bortnik, T. P. O'Brien, J. F. Fennell, and J. B. Blake (2020a), Empirically estimated electron lifetimes in the Earth's radiation belts: Comparison with theory, *Geophys. Res. Lett.*, *47*(3), e2019GL086,056, doi: https://doi.org/10.1029/2019GL086056.

Claudepierre, S. G., Q. Ma, J. Bortnik, T. P. O'Brien, J. F. Fennell, and J. B. Blake (2020b), Empirically Estimated Electron Lifetimes in the Earth's Radiation Belts: Van Allen Probe Observations, *Geophys. Res. Lett.*, *47*(3), e2019GL086,053, doi: https://doi.org/10.1029/2019GL086053.

Clilverd, M. A., D. Nunn, S. J. Lev-Tov, U. S. Inan, R. L. Dowden, C. J. Rodger, and A. J. Smith (2002), Determining the size of lightning-induced electron precipitation pathes, *J. Geophys. Res.*, *107*(A8), 1168, doi:10.1029/2001JA000301.

Clilverd, M. A., C. J. Rodger, and D. Nunn (2004), Radiation belt electron precipitation fluxes associated with lightning, *J. Geophys. Res.*, *109*, A12208, doi: 10.1029/2004JA010644.

Clilverd, M. A., C. J. Rodger, T. Ulich, A. Seppälä, E. Turunen, A. Botman, and N. R. Thomson (2005), Modeling a large solar proton event in the southern polar atmosphere, *Journal of Geophysical Research: Space Physics*, *110*, A09307.

Cotts, B. R. T. (2011), Global quantification of lightning-induced electron precipition using very low frequency remote sensing, Ph.D. thesis, Stanford University.

Cummins, K. L., E. P. Krider, and M. D. Malone (1998), The US national lightning detection network^{TM} and applications of cloud-to-ground lightning data by electric power utilities, *IEEE Trans. on Elect. Comp.*, *40*, 465–480, doi:10.1109/15.736207.

Dowden, R. L., J. B. Brundell, and C. J. Rodger (2002), VLF lightning location by time of group arrival (TOGA) at multiple sites, *Journal of Atmospheric and Solar-Terrestrial Physics*, *64*(7), 817–830.

Dungey, J. (1963), Loss of Van Allen electrons due to whistlers, *Planetary and Space Science*, *11*(6), 591–595.

Fang, X., C. E. Randall, D. Lummerzheim, W. Wang, G. Lu, S. C. Solomon, and R. A. Frahm (2010), Parameterization of monoenergetic electron impact ionization, *Geophys. Res. Lett.*, *37*, L22106.

Glukhov, V. S., V. P. Pasko, and U. S. Inan (1992), Relaxation of transient lower ionospheric disturbances caused by lightning-whister-induced electron precipitation bursts, *J. Geophys. Res.*, *97*(A11), 16,971–16,979.

Golden, D. I., M. Spasojevic, F. R. Foust, N. G. Lehtinen, N. P. Meredith, and U. S. Inan (2010), Role of the plasmapause in dictating the ground accessibility of ELF/VLF chorus, *J. Geophys Res.*, *115*, A11211.

Graf, K. L., M. Spasojevic, R. A. Marshall, N. G. Lehtinen, F. R. Foust, and U. S. Inan (2013a), Extended lateral heating of the nighttime ionosphere by ground-based VLF transmitters, *J. Geophys. Res.*, *118*(12), 7783–7797, doi:https://doi.org/10.1002/2013JA019337.

Graf, K. L., N. G. Lehtinen, M. Spasojevic, M. B. Cohen, R. A. Marshall, and U. S. Inan (2013b), Analysis of experimentally-validated trans-ionospheric attenuation estimates of VLF signals, *J. Geophys. Res.*, *118*(5), 2708–2720, doi:https://doi.org/10.1002/jgra.50228.

Helliwell, R. A. (1965), *Whistlers and Related Ionospheric Phenomena*, Stanford University Press.

Helliwell, R. A., J. P. Katsufrakis, and M. Trimpi (1973), Whistler-induced amplitude perturbation in VLF propagation, *J. Geophys. Res.*, *78*(22), 4679–4688.

Hendry, A. T., A. Seppälä, C. J. Rodger, and M. A. Clilverd (2021), Impact of EMIC-wave driven electron precipitation on the radiation belts and the atmosphere, *Journal of Geophysical Research: Space Physics*, p. e2020JA028671, doi:10.1029/2020JA028671.

Houze, R. A., K. L. Rasmussen, M. D. Zuluaga, and S. R. Brodzik (2015), The variable nature of convection in the tropics and subtropics: A legacy of 16 years of the tropical rainfall measuring mission satellite, *Reviews of Geophysics*, *53*(3), 994–1021.

Inan, U. S. (1977), Non-linear gyroresonant interactions of energetic particles and coherent VLF waves in the magnetosphere, Ph.D. thesis, stanford university.

Inan, U. S., and D. L. Carpenter (1986), On the correlation of whistlers and associated subionospheric VLF/LF perturbations, *J. Geophys. Res.*, *91*(A3), 3106–3116.

Inan, U. S., and D. L. Carpenter (1987), Lightning-induced electron precipitation events observed at L=2.4 as phase and amplitude perturbations on subionospheric VLF signals, *J. Geophys. Res.*, *92*(A4), 3293–3303.

Inan, U. S., D. L. Carpenter, R. A. Helliwell, and J. P. Katsufrakis (1985), Subionospheric VLF/LF phase perturbations produced by lightning-whistler induced particle precipitation, *J. Geophys. Res.*, *90*(A8), 7457–7469.

Inan, U. S., D. Piddyachiy, W. B. Peter, J. A. Sauvaud, and M. Parrot (2007), DEMETER satellite observations of lightning-induced electron precipitation, *Geophys. Res. Lett.*, *34*(7), L07103, doi:https://doi.org/10.1029/2006GL029238.

Inan, U. S., S. A. Cummer, and R. A. Marshall (2010), A survey of ELF and VLF research on lightning-ionosphere interactions and causative discharges, *J. Geophys Res.*, *115*, A00E36, doi:10.1029/2009JA014775.

Johnson, M. P., U. S. Inan, S. J. Lev-Tov, and T. F. Bell (1999), Scattering pattern of lightning-induced ionospheric disturbances associated with early/fast VLF events, *Geophys. Res. Lett.*, *26*(15), 2363–2366.

Lauben, D. S., U. S. Inan, and T. F. Bell (1999), Poleward-displaced electron precipitation from lightning-generated oblique whisters, *Geophys. Res. Lett.*, *26*(16), 2633–2636.

Lehtinen, N. G., and U. S. Inan (2007), Possible persistent ionization caused by giant blue jets, *Geophys. Res. Lett.*, *34*, L08804, doi:10.1029/2006GL029051.

Lehtinen, N. G., T. F. Bell, and U. S. Inan (1999), Monte Carlo simulation of runaway MeV electron breakdown with application to red sprites and terrestrial gamma ray flashes, *J. Geophys. Res.*, *104*(A11), 24,699–24,712.

Lohrey, B., and A. B. Kaiser (1979), Whistler-induced anomalies in VLF propagation, *J. Geophys. Res.*, *84*(A9), 5121–5130.

Marshall, R., W. Xu, A. Sousa, M. McCarthy, and R. Millan (2019a), X-ray signatures of lightning-induced electron precipitation, *Journal of Geophysical Research: Space Physics*, *124*(12), 10,230–10,245.

Marshall, R. A. (2012), An improved model of the lightning electromagnetic field interaction with the D-region ionosphere, *J. Geophys Res.*, *117*, A03316, doi: https://doi.org/10.1029/2011JA017408.

Marshall, R. A., U. S. Inan, and V. S. Glukhov (2010), Elves and associated electron density changes due to cloud-to-ground and in-cloud lightning discharges, *J. Geophys. Res.*, *115*, A00E17, doi:10.1029/2009JA014469.

Marshall, R. A., W. Xu, A. Kero, R. Kabirzadeh, and E. Sanchez (2019b), Atmospheric effects of a relativistic electron beam injected from above: chemistry, electrodynamics, and radio scattering, *Frontiers in Astronomy and Space Sciences*, *6*, 6.

Marshall, R. A., W. Xu, T. Woods, C. Cully, A. Jaynes, C. Randall, D. Baker, M. McCarthy, H. E. Spence, G. Berland, et al. (2020), The AEPEX mission: Imaging energetic particle precipitation in the atmosphere through its bremsstrahlung X-ray signatures, *Advances in Space Research*, *66*(1), 66–82.

Meng, C. (1976), Simultaneous observations of low-energy electron precipitation and optical auroral arcs in the evening sector by the DMSP 32 satellite, *J. Geophys. Res.*, *81*, 2771–2785.

Pasko, V. P., U. S. Inan, T. F. Bell, and Y. N. Taranenko (1997), Sprites produced by quasi-electrostatic heating and ionization in the lower ionosphere, *J. Geophys. Res.*, *102*(A3), 4529–4561.

Peter, W. B. (2007), Quantitative measurement of lightning-induced electron precipitation using VLF remote sensing, Ph.D. thesis, Stanford University.

Peter, W. B., and U. S. Inan (2007), A quantitative comparison of lightning-induced electron precipitation and VLF signal perturbations, *J. Geophys. Res.*, *112*, A12212, doi: 10.1029/2006JA012165.

Rakov, V. A. (2016), *Fundamentals of lightning*, Cambridge University Press.

Randall, C. E., V. L. Harvey, C. S. Singleton, S. M. Bailey, P. F. Bernath, M. Codrescu, H. Nakajima, and J. M. Russell III (2007), Energetic particle precipitation effects on the southern hemisphere stratosphere in 1992–2005, *J. Geophys. Res.*, *112*(D8), D08308, doi: https://doi.org/10.1029/2006JD007696.

Rees, M. H. (1992), Auroral energy deposition rate, *Planet. Space Sci.*, *40*(2/3), 299–313.

Rodger, C. J. (2003), Subionospheric VLF perturbations associated with lightning discharges, *J. Atmos. Solar-Terr. Phys.*, *65*(5), 591–606.

Rodger, C. J., M. A. Clilverd, and R. J. McCormick (2003), Significance of lightning-generated whistlers to inner radiation belt electron lifetimes, *J. Geophys. Res.*, *108*, 1462, doi:https://doi.org/10.1029/2003JA009906.

Rodger, C. J., R. J. McCormick, and M. A. Clilverd (2004), Testing the importance of precipitation loss mechanisms in the inner radiation belt, *Geophys. Res. Lett.*, *31*, L10803, doi:https://doi.org/10.1029/2004GL019501.

Rodger, C. J., M. A. Clilverd, N. R. Thomson, D. Nunn, and J. Lichtenberger (2005), Lightning driven inner radiation belt energy deposition into the atmosphere: regional and global estimates, *Ann. Geophys.*, *23*, 3419–3430.

Rodger, C. J., C.-F. Enell, E. Turunen, M. A. Clilverd, N. R. Thomson, and P. T. Verronen (2007), Lightning-driven inner radiation belt energy deposition into the atmosphere: implications for ionisation-levels and neutral chemistry, *Ann. Geophys.*, *25*(8), 1745–1757, doi:10.5194/angeo-25-1745-2007.

Rusch, D., J.-C. Gérard, S. Solomon, P. Crutzen, and G. Reid (1981), The effect of particle precipitation events on the neutral and ion chemistry of the middle atmosphere–I. odd nitrogen, *Planetary and Space Science*, *29*(7), 767–774, doi:http://dx.doi.org/10.1016/0032-0633(81)90048-9.

Rycroft, M. J. (1973), Enhanced energetic electron intensities at 100 km altitude and a whistler propagating through the plasmasphere, *Planet. Space. Sci.*, *21*(2), 239–251.

Seppälä, A., E. Douma, C. J. Rodger, P. T. Verronen, M. A. Clilverd, and J. Bortnik (2018), Relativistic electron microburst events: Modeling the atmospheric impact, *Geophys. Res. Lett.*, *45*(2), 1141–1147.

Sinnhuber, M., H. Nieder, and N. Wieters (2012), Energetic particle precipitation and the chemistry of the mesosphere/lower thermosphere, *Surveys in Geophysics*, *33*(6), 1281–1334.

Solomon, S., D. Rusch, J. Gérard, G. Reid, and P. Crutzen (1981), The effect of particle precipitation events on the neutral and ion chemistry of the middle atmosphere: II. odd hydrogen, *Planetary and Space Science*, *29*(8), 885–893, doi:http://dx.doi.org/10.1016/0032-0633(81)90078-7.

Sousa, A. P. (2018), Global and seasonal effects of lightning-induced electron precipitation, Ph.D. thesis, Stanford University.

Stolzenburg, M. (1994), Observations of high ground flash densities of positive lightning in summertime thunderstorms, *Monthly weather review*, *122*(8), 1740–1750.

Thébault, E., et al. (2015), International geomagnetic reference field: the 12th generation, *Earth, Planets and Space*, *67*(1), 1–19.

Thorne, R. M. (1980), The importance of energetic particle precipitation on the chemical composition of the middle atmosphere, *pure and applied geophysics*, *118*(1), 128–151.

Tobiska, W. K., and S. D. Bouwer (2006), New developments in solar2000 for space research and operations, *Adv. Space Res.*, *37*, 347–358, doi:10.1016/j.asr.2005.08.015.

Turunen, E., H. Matveinen, J. Tolvanen, and H. Ranta (1996), D-region ion chemistry model, in *STEP Handbook of Ionospheric Models*, edited by R. W. Schunk, pp. 1–25, SCOSTEP Secretariat, Boulder, Colorado.

Turunen, E., P. T. Verronen, A. Seppälä, C. J. Rodger, M. A. Clilverd, J. Tamminen, C.-F. Enell, and T. Ulich (2009), Impact of different energies of precipitating particles on NOx generation in the middle and upper atmosphere during geomagnetic storms, *Journal of Atmospheric and Solar-Terrestrial Physics*, *71*(10), 1176–1189.

Turunen, E., A. Kero, P. T. Verronen, Y. Miyoshi, S.-I. Oyama, and S. Saito (2016), Mesospheric ozone destruction by high-energy electron precipitation associated with pulsating aurora, *Journal of Geophysical Research: Atmospheres*, *121*(19), 11,852–11,861, doi: https://doi.org/10.1002/2016JD025015.

Verronen, P. T. (2006), Ionosphere-atmosphere interaction during solar proton events, Ph.D. thesis, Univ. of Helsinki, Helsinki, Finland.

Verronen, P. T., A. Seppälä, M. A. Clilverd, C. J. Rodger, E. Kyrölä, C.-F. Enell, T. Ulich, and E. Turunen (2005), Diurnal variation of ozone depletion during the October–November 2003 solar proton events, *J. Geophys. Res.*, *110*, A09S32, doi: 10.1029/2004JA010932.

Verronen, P. T., M. E. Andersson, D. R. Marsh, T. Kovacs, and J. M. C. Plane (2016), WACCM-D—Whole Atmosphere Community Climate Model with D-region ion chemistry, *J. Adv. Modeling Earth Sys.*, *8*(2), 945–975.

Vette, J. I. (1991), The AE-8 trapped electron model environment, *Tech. Rep. 24*, National Space Science Data Center (NSSDC) World Data Center A for Rockets and Satellites (WDC-A-R&S).

Voss, H. D., W. L. Imhof, M. Walt, J. Mobilia, E. E. Gaines, J. B. Reagan, and U. S. Inan (1984), Lightning induced electron precipitation, *Nature*, *312*, 740–742.

Voss, H. D., M. Walt, W. L. Imhof, J. Mobilia, and U. S. Inan (1998), Satellite observations of lightning-induced electron precipitation, *J. Geophys. Res.*, *103*, 11,725–11,744.

Xu, W., and R. A. Marshall (2019), Characteristics of Energetic Electron Precipitation Estimated from Simulated Bremsstrahlung X-ray Distributions, *Journal of Geophysical Research: Space Physics*, *124*(4), 2831–2843.

Xu, W., R. A. Marshall, X. Fang, E. Turunen, and A. Kero (2018), On the effects of bremsstrahlung radiation during energetic electron precipitation, *Geophys. Res. Lett.*, *45*, 1167–1176.

Xu, W., R. A. Marshall, A. Kero, E. Turunen, D. Drob, J. Sojka, and D. Rice (2019), VLF measurements and modeling of the D-region response to the 2017 total solar eclipse, *IEEE Transactions on Geoscience and Remote Sensing*, *57*(10), 7613–7622.

Xu, W., R. A. Marshall, H. N. Tyssøy, and X. Fang (2020), A Generalized Method for Calculating Atmospheric Ionization by Energetic Electron Precipitation, *Journal of Geophysical Research: Space Physics*, *125*(11), e2020JA028,482.